Dual Band Radiation Pattern Reconfigurable Antenna for Two-Port 5G Mobile Terminals

Surentiran Padmanathan[1], Azremi Abdullah Al-Hadi[1], Samir Salem Al-Bawri[2], Ping Jack Soh[1,3]
[1]Advanced Communication Engineering (ACE) Center of Excellence, Faculty of Electronic Engineering Technology, Universiti Malaysia Perlis, 02600 Arau, Perlis, MALAYSIA.
[2]Space Science Centre, Institute of Climate Change, Universiti Kebangsaan Malaysia (UKM), Bangi 43600, MALAYSIA.
[3]Centre for Wireless Communications (CWC), University of Oulu, Erkki Koiso-Kanttilan Katu 3, 90570 Oulu, FINLAND.
[1]suren.wgen@hotmail.com

***Abstract* — In this paper, a dual band radiation pattern reconfigurable antenna for 5G mobile terminals is presented. Two identical PIFA elements are connected to a PIN diode and feeding port to enable reconfiguration. Copper strips are used as RF switches in this antenna design to represent the actual PIN diodes. The switching of the two PIFA elements in sequence enabled the radiation pattern reconfiguration in two frequency bands, with 6dB impedance bandwidth ranging from 3.8 to 18 GHz. Besides that, this antenna features high isolation and low envelope correlation coefficient due to the low mutual coupling between the two ports. These advantages make the antenna promising for application in future 5G mobile terminals.**

Keywords — ***reconfigurable antennas, dualband antennas, radiation pattern reconfiguration, MIMO antennas, mobile terminals.***

I. Introduction

Due to the effectiveness in providing greater channel capacity in multipath environments, the adoption of Multiple Input Multiple Output (MIMO) technology in 4th Generation (4G) Long-Term Evolution (LTE) and Long-Term Evolution Advanced (LTE-A) has shown a great achievement in mobile communication. In addition to this, the 3rd Generation Partnership Project (3GPP) recently approved the 5G New Radio (NR) standard, ushering in a new era in mobile communication systems [1]. As a result, higher frequency spectrums are needed to support higher data rates, reliable connectivity, and the additional services envisioned in future 5G applications [2, 3]. Thus, telco industries are looking forward to enhance the antenna designs for mobile terminal to provide multigigabits per second (Gbps) of connectivity.

Due to the use of MIMO technology to transmit and receive information with high data rates, integrating multiple antenna elements in mobile terminals to accommodate additional 5G bands will be very challenging. This is due to space constraints in mobile terminals, where closely spaced multiple antenna elements directly results in increased correlation and information loss [4]. Thus, antenna miniaturization and the ability to operate in multiple frequency bands has become an underlying need to fulfill the requirements of 5G mobile terminals [5]. Furthermore, when implementing micro cells in 5G, the beams generated by these antenna elements should be high in gain and highly directive to mitigate multipath fading and pathloss caused by various environmental conditions.

Replacing conventional multiple antenna structures (MAS) in MIMO mobile terminals with reconfigurable antennas is a promising solution in overcoming these issues [6]. They can either reconfigure their radiation pattern, operating frequency and polarization or any combinations of them. Radiation pattern reconfiguration mitigates multipath fading effect in rich scattering environments by reconfiguring the antenna's null beam towards the direction of noise [7]. Beam reconfiguration can be performed either using RF switches such as RF microelectromechanical switches (RF-MEMS), PIN diodes, or varactor diodes [8-11]. Activating and deactivating RF switches alters the impedance and electrical length of the antenna, resulting in the desired reconfigurable properties.

Since reconfigurable antennas are more advantageous compared to passive antennas in 5G MIMO applications, a dual band, two-port radiation pattern reconfigurable antenna is proposed in this work for 5G mobile terminals. This two-port antenna is able to achieve dual band while performing radiation pattern reconfiguration. Moreover, it has the capability to achieve wide bandwidth which lies between 11 GHz to 18 GHz, that can be utilized for future 5G applications. This antenna design is developed based on prove of concept method and therefore copper strips have been used as the artificial RF switches to replace the actual PIN diodes. To best of our knowledge, this technique efficiently utilizes the space in mobile terminal to achieve dual band at sub-6 GHz and > 6 GHz region while performing radiation pattern reconfiguration together. It is important to note that available MIMO antennas in literature are only able to reconfigure their radiation pattern in a single band at sub-6 GHz region [12-14]. This paper is organized as follows. Section II describes the antenna design and detailed dimensions, followed by the results presentation and discussion in Section III. Finally, this research is summarized in Section IV.

II. Antenna Design

Fig. 1 shows the proposed antenna design. This antenna was modeled and simulated in Computer Simulation Tool (CST)

software. Two identical PIFA elements (PIFA 1 and PIFA 2) are designed with a patch length, *L*, and width, *W*, of 8 mm and 3.3 mm, respectively. They are integrated orthogonally to form the proposed antenna, and each of this dual-PIFA structure is placed at the top left and right corners of a 120mm x 60mm x 1.575mm RT/Duroid 5880 substrate, as shown in Fig. 1(a). A ground plane with the size of 120mm x 60mm x 0.035mm is etched on the substrate's bottom layer, as shown in Fig. 1(b).

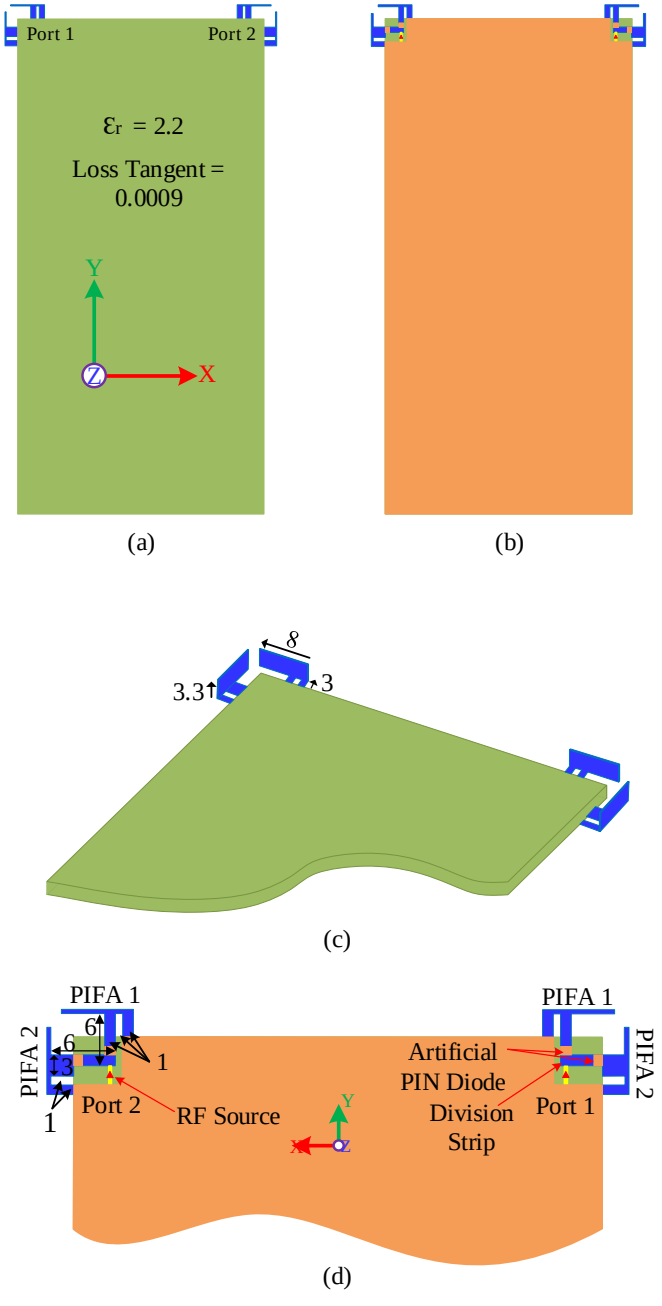

Fig. 1. The geometry of the proposed antenna. (a) front view (b) rear view (c) perspective view (d) closeup rear view. All dimensions are millimeter (mm).

The detailed dimensions of the PIFA structures are illustrated in Fig. 1(c). As shown in Fig. 1(d), two PIFA elements fed by the same RF port, which is placed on the same surface with ground plane. To reconfigure the patterns, only one PIFA element (either PIFA 1 or 2) is activated at a certain time as the main radiator, whereas the other element acts as a parasitic element. The presence of the copper strip on the feeding strip (ON state) will allow the RF current to flow through, activating the connected PIFA element as main radiator. On the contrary, RF current will be disconnected due to the non-existence of copper strip (OFF state) at this location. Hence, changing the activation of the PIFA element as main radiator within the same port will produce the radiation pattern and frequency reconfiguration. Moreover, the coupling between the two PIFA elements within the same port enables its multiband behavior due to the common ground plane shared by both elements.

III. Results & Discussion

The antenna is simulated by activating the same PIFA element (either PIFA 1 or 2) at both ports simultaneously. The S-parameters illustrated in Fig. 2 indicates dual band operation for both PIFA elements with at least -6 dB of reflection coefficient (S_{11} or S_{22}). The first band is centered at 4 GHz, whereas the second band operates with wider bandwidth (from 11 to 18 GHz). When PIFA element 1 is activated as the driven element, the dual band operation is centered at 4.25 GHz and 11.7 GHz with a bandwidth of 480 MHz and 4 GHz, respectively. On the other hand, when PIFA element 2 is driven, the dual band operation is centered at 4.12 GHz and 11.7 GHz with a bandwidth of 430 MHz and 6.95 GHz, respectively. Transmission coefficients (S_{21} and S_{12}) of less than – 8 dB and -12 dB are seen between ports in the first and second band, respectively. This indicates good isolation and low mutual coupling.

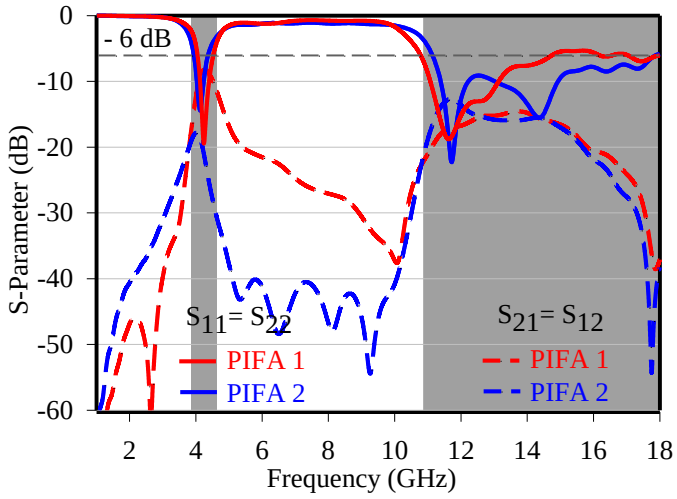

Fig. 2. Simulated S-parameters for PIFA 1 and 2 at both ports.

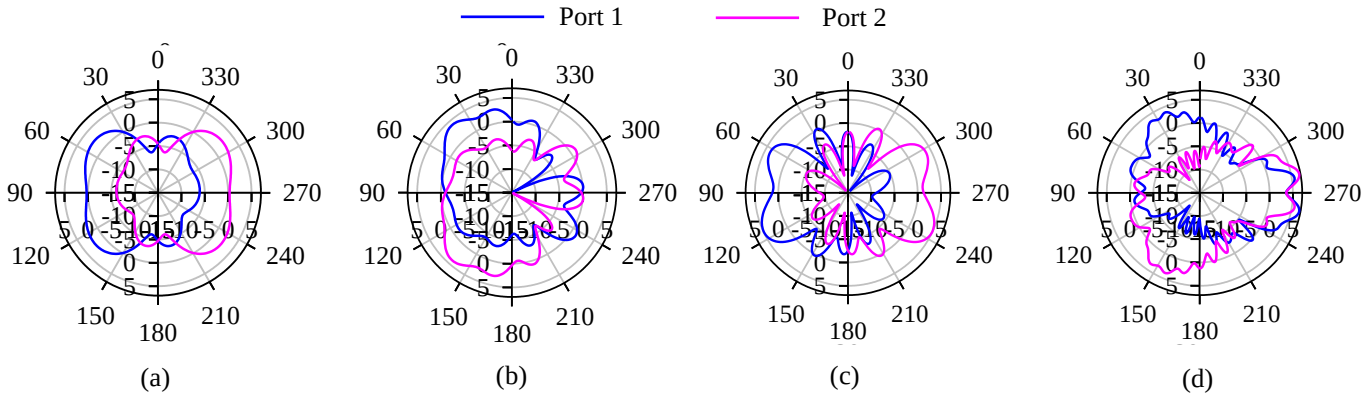

Fig. 3. Simulated two-dimensional radiation patterns of PIFA element 1. (a) xz-plane at 4.25 GHz, (b) xy-plane at 4.25 GHz , (c) xz-plane at 11.7 GHz and (b) xy-plane at 11.7 GHz .

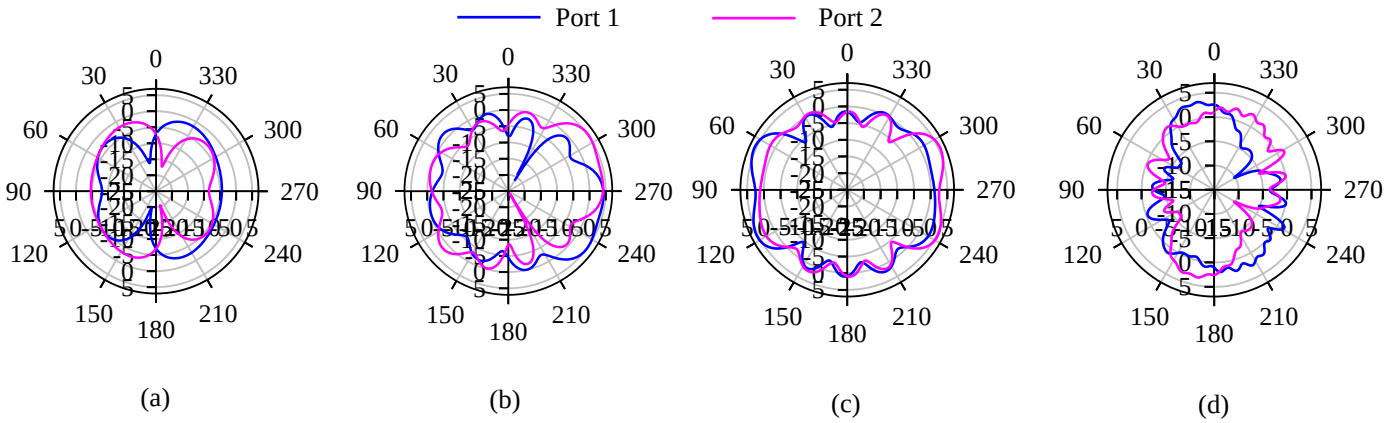

Fig. 4. Simulated two-dimensional radiation patterns of PIFA element 2: (a) xz-plane at 4.12 GHz, (b) xy-plane at 4.12 GHz , (c) xz-plane at 11.7 GHz and (b) xy-plane at 11.7 GHz.

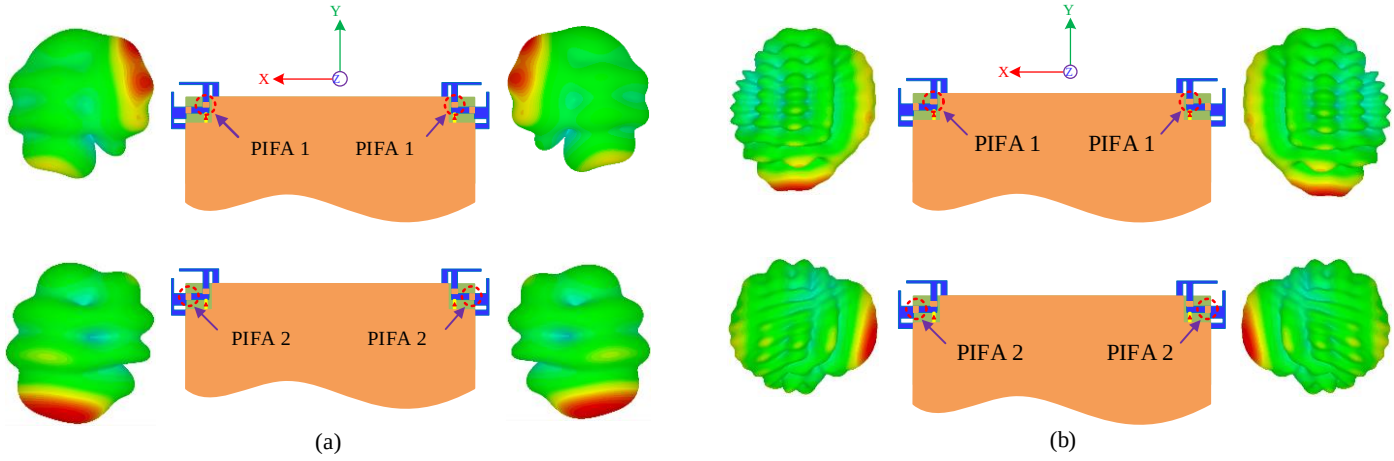

Fig. 5. Simulated three-dimensional radiation patterns of the proposed antenna observed at (a) 4.16 GHz and (b) 11.7 GHz when the same PIFA elements are activated at both ports

TABLE I
THE PIFA ELEMENT CONFIGURATION AT BOTH PORT 1 AND PORT 2

PIFA Elements	PIFA 1	PIFA 2	Resonance Frequency (f_c)	Bandwidth (MHz)	Main Lobe Gain (dB)
Status of the PIFA elements at both ports	**Radiator**	Parasitic	4.25 GHz	480	2.04
			11.7 GHz	4000	6.42
	Parasitic	**Radiator**	4.12 GHz	430	3.12
			11.7 GHz	6950	5.13

Fig. 3 presents the simulated two-dimensional radiation patterns of PIFA element 1 at 4.25 GHz and 11.7 GHz. On the other hand, the simulated two-dimensional radiation patterns of PIFA element 2 at 4.12 GHz and 11.7 GHz are depicted in Fig. 4. These results are illustrated at both xz-plane and xy-plane. It can be noticed that PIFA element 1 has a maximum main lobe gain of 2.04 dB and 6.42 dB in the xy-plane at 4.25 GHz and 11.7 GHz, respectively. On the other hand, PIFA element 2 has a maximum main lobe gain of 3.12 dB and 5.13 dB in the xy-plane and xz-plane at 4.12 GHz and 11.7 GHz, respectively. The details of the achieved resonant frequencies are described in Table I. The achievement of identical resonant frequency between PIFA element 1 and PIFA element 2 is essential to observe the radiation pattern reconfiguration. Due to the existence of mutual coupling between PIFA element 1 and 2 at each port, identical frequencies are successfully attained. Thus, radiation pattern reconfiguration is successfully observed at these frequencies. In addition, the perpendicular arrangement of the PIFA elements directs the radiation pattern towards different direction, enabling reconfiguration of beams at the 4.16 GHz and 11.7 GHz.

Fig. 5 illustrates the three-dimensional radiation patterns observed at 4.16 GHz and 11.7 GHz. It is validated that the proposed antenna reconfigures its beams when the switch is activated to drive the different PIFA elements (PIFA 1 and PIFA 2). When the PIFA elements are activated in sequent at port 1, the observation at 4.16 GHz indicates that the main lobe direction of PIFA element 1 is directed towards 44˚ and PIFA element 2 is directed towards 235˚ in the xy-plane. On the other hand, at port 2, the main lobe direction of PIFA element 1 and PIFA element 2 is directing towards 136˚ and 304˚, respectively in the xy-plane. At 11.7 GHz, it can be observed that the main lobe direction of PIFA element 1 and PIFA element 2 at port 1 is directed towards 259˚ and 11˚, respectively in the xy-plane. On the other hand, the main lobe direction of PIFA element 1 and PIFA element 2 at port 2 is directed towards 281˚ and 169˚, respectively in the xy-plane. It can be concluded that the proposed antenna is able to reconfigure its radiation patterns towards at least four different directions at each identical frequency.

Envelop Correlation Coefficient (ECC) is the value of correlation between multiple antenna elements in a mobile terminal, which used to measure the MIMO diversity performance. A MIMO antenna system which has ECC value of less than 0.5 is able operate with low correlation and good diversity performance. Simulation results shown in Fig. 7 indicates ECC values of less than 0.2 for PIFA element 1 and 2 are achieved across the respective resonant bands. This is due to the different main lobe directions from each PIFA elements. Furthermore, the compactness of the PIFA elements and their larger space between two ports contributed to the low levels of correlations.

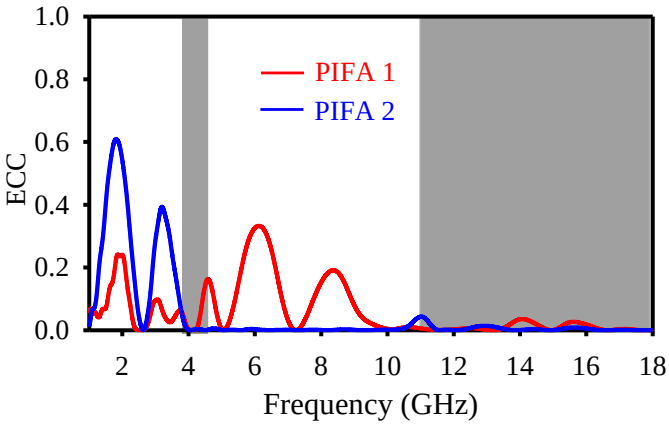

Fig. 7. Simulated ECC between port 1 and port 2 for PIFA element 1 and PIFA element 2.

IV. CONCLUSION

In this paper, a dual band radiation pattern reconfigurable antenna is proposed for two-port 5G MIMO mobile terminals. The PIFA elements of this antenna operated in the first band centered at 4 GHz, and the second between 11 and 18 GHz with at least -6 dB of reflection coefficient. The reconfiguration of radiation pattern was performed effectively as each PIFA element from both ports are able to lead the radiation towards various directions. Besides that, the transmission coefficient and ECC values of less than –10 dB and 0.5, respectively, indicates that a good isolation and low mutual coupling. From these results, the proposed MIMO antenna can be potentially suitable for 5G mobile terminal applications.

REFERENCES

[1] H. Hu, H. Gao, Z. Li, and Y. Zhu, "A sub 6GHz massive MIMO system for 5G new radio," in *2017 IEEE 85th Vehicular Technology Conference (VTC Spring)*, 2017, pp. 1-5.

[2] A. Al-Dulaimi, S. Al-Rubaye, Q. Ni, and E. Sousa, "5G communications race: Pursuit of more capacity triggers LTE in unlicensed band," *IEEE vehicular technology magazine*, vol. 10, pp. 43-51, 2015.

[3] M. S. Sharawi, M. Ikram, and A. Shamim, "A two concentric slot loop based connected array MIMO antenna system for 4G/5G terminals," *IEEE Transactions on antennas and propagation*, vol. 65, pp. 6679-6686, 2017.

[4] Y.-L. Ban, C. Li, G. Wu, and K.-L. Wong, "4G/5G multiple antennas for future multi-mode smartphone applications," *IEEE access*, vol. 4, pp. 2981-2988, 2016.
[5] Y. Li, Y. Luo, and G. Yang, "Multiband 10-antenna array for sub-6 GHz MIMO applications in 5-G smartphones," *IEEE access*, vol. 6, pp. 28041-28053, 2018.
[6] J. Costantine, Y. Tawk, S. E. Barbin, and C. G. Christodoulou, "Reconfigurable antennas: Design and applications," *Proceedings of the IEEE*, vol. 103, pp. 424-437, 2015.
[7] N. H. Chamok, M. H. Yılmaz, H. Arslan, and M. Ali, "High-gain pattern reconfigurable MIMO antenna array for wireless handheld terminals," *IEEE Transactions on Antennas and Propagation*, vol. 64, pp. 4306-4315, 2016.
[8] X. Meng, "Small-size eight-band frequency reconfigurable antenna loading a MEMS switch for mobile handset applications," *International Journal of Antennas and Propagation*, vol. 2014, 2014.
[9] Y. Liu, P. Liu, Z. Meng, L. Wang, and Y. Li, "A planar printed nona-band loop-monopole reconfigurable antenna for mobile handsets," *IEEE Antennas and Wireless Propagation Letters*, vol. 17, pp. 1575-1579, 2018.
[10] F. A. Asadallah, J. Costantine, and Y. Tawk, "A multiband compact reconfigurable PIFA based on nested slots," *IEEE antennas and wireless propagation letters*, vol. 17, pp. 331-334, 2018.
[11] W.-W. Lee and Y.-S. Cho, "Frequency tunable antenna using coupling patterns for mobile terminals," *Electronics Letters*, vol. 51, pp. 1725-1726, 2015.
[12] I. Syrytsin, H. A. Vesterager, S. B. Nørgaard, L. Thomsen, S. C. Del Barrio, and G. F. Pedersen, "Pattern-reconfigurable mobile terminal antenna system for MIMO and link stabilization in LTE," 2018.
[13] F. A. Asadallah, J. Costantine, Y. Tawk, R. Kanj, Z. Ghorayeb, T. Al-Bahar, *et al.*, "An antenna system with a voice-controlled personalized switchable radiation coverage," *IEEE Antennas and Wireless Propagation Letters*, vol. 17, pp. 693-696, 2018.
[14] C. Rhee, Y. Kim, T. Park, S.-s. Kwoun, B. Mun, B. Lee, *et al.*, "Pattern-reconfigurable MIMO antenna for high isolation and low correlation," *IEEE Antennas and Wireless Propagation Letters*, vol. 13, pp. 1373-1376, 2014.